Author(s): Ketolainen, T. & Havu, V. & Puska, Martti J.

Title: Enhancing conductivity of metallic carbon nanotube networks by transition metal adsorption

Year: 2015

Version: Final published version

Please cite the original version:

Ketolainen, T. & Havu, V. & Puska, Martti J. 2015. Enhancing conductivity of metallic carbon nanotube networks by transition metal adsorption. The Journal of Chemical Physics. Volume 142, Issue 5. 054705/1-9. ISSN 1089-7690 (electronic). DOI: 10.1063/1.4907205.

Enhancing conductivity of metallic carbon nanotube networks by transition metal adsorption

T. Ketolainen, V. Havu, and M. J. Puska

Citation: The Journal of Chemical Physics **142**, 054705 (2015); doi: 10.1063/1.4907205
View online: http://dx.doi.org/10.1063/1.4907205
View Table of Contents: http://scitation.aip.org/content/aip/journal/jcp/142/5?ver=pdfcov
Published by the AIP Publishing

Enhancing conductivity of metallic carbon nanotube networks by transition metal adsorption

T. Ketolainen,[a] V. Havu, and M. J. Puska
COMP, Department of Applied Physics, Aalto University, P.O. Box 11100, FI-00076 Aalto, Finland

(Received 11 November 2014; accepted 14 January 2015; published online 5 February 2015)

The conductivity of carbon nanotube thin films is mainly determined by carbon nanotube junctions, the resistance of which can be reduced by several different methods. We investigate electronic transport through carbon nanotube junctions in a four-terminal configuration, where two metallic single-wall carbon nanotubes are linked by a group 6 transition metal atom. The transport calculations are based on the Green's function method combined with the density-functional theory. The transition metal atom is found to enhance the transport through the junction near the Fermi level. However, the size of the nanotube affects the improvement in the conductivity. The enhancement is related to the hybridization of chromium and carbon atom orbitals, which is clearly reflected in the character of eigenstates near the Fermi level. The effects of chromium atoms and precursor molecules remaining adsorbed on the nanotubes outside the junctions are also examined. © *2015 AIP Publishing LLC.* [http://dx.doi.org/10.1063/1.4907205]

I. INTRODUCTION

Various new electronic devices utilizing carbon nanotube (CNT) thin films have been introduced during the last few years. For instance, the CNT thin films are promising component materials for transistors,[1] organic light-emitting diodes,[2] displays,[3] and solar cells.[4] The most important advantage of the CNT thin films is that they are both conductive and transparent as well as flexible. Therefore, they have been proposed to be used as transparent electrodes. However, a great challenge in the fabrication of CNT thin films is to achieve high transparency together with high film conductivity.[5] The film conductivity depends on the structure of the network that the CNTs form.[6] More recent studies have shown that the highest resistance in the CNT thin film comes from the nanotube junctions.[7] Thus, it is important to consider the transport properties of the CNT junctions in order to understand the conductivity of the whole thin film. A real CNT thin film may be formed by CNT bundles, and the conductivity of the whole film is determined by the properties of CNT bundles.[8] For instance, the film conductivity depends both on the bundle diameter and the number density of interbundle junctions.[9]

A nanotube network usually contains both metallic and semiconducting CNTs. The semiconducting nanotubes increase the resistivity and change the transport mechanism in the CNT thin film.[10] Experimental studies of crossed CNT junctions have shown that the conductance of a junction is much lower when the other nanotube is semiconducting.[11] The conductance of the CNT junction also depends on the arrangement of carbon atoms in the junction region,[12] the angle between the nanotubes,[13–15] and pressure applied to the junction.[16–18]

A few different methods to reduce the resistivity of CNT thin films have been reported recently.[19] Treating the nanotube network with acids enhances the conductivity by lowering the resistance of CNT junctions.[20] The effect of the acid treatment on the conductivity of a CNT thin film has been found to be stronger when the nanotubes form a honeycomb-like network rather than being randomly oriented.[21] Organic molecules connecting the ends of the CNTs make it possible to build a junction that is almost completely transparent.[22] The structure of the linker molecule, however, affects the transport remarkably. Another promising method to lower the sheet resistance could be nanosoldering the nanotube junctions with palladium.[23] In addition, a weak external potential that can be induced, e.g., by impurities in a CNT network leads to an increase in the conductance of a CNT junction by allowing momentum exchange with the environment.[24] The effect is remarkable when the two CNTs in the junction are of different chirality. Furthermore, previous density-functional theory (DFT) calculations indicate that the conductance of a metallic CNT junction can be improved by linking the nanotubes with gold nanoparticles.[25] This has also been confirmed in an experimental study.[26]

Experimentally, it has been shown that transition metal (TM) atoms reduce the junction resistance efficiently.[27,28] In particular, chromium linker atoms enhance the conductance of the junction significantly. Group 6 TM atoms chromium, molybdenum, and tungsten possess six valence electrons and these atoms obtain a closed-shell structure when they bind to two carbon sidewall hexagons in CNT junctions. In a recent study, DFT calculations have shown that the electronic transport through a junction consisting of two parallel semi-infinite (5,5) CNTs can be improved by linking the CNTs with a metal atom.[29]

In this article, we consider a CNT junction where two metallic *perpendicular* and *infinite* CNTs are connected by a group 6 TM atom. Other TM atoms have not been considered because in the CNT junction they do not result in a stable closed-shell structure and the electron transport mechanism is expected to be remarkably different. DFT calculations are

[a]Electronic mail: tomi.ketolainen@aalto.fi

carried out in order to examine the transport in the CNT junction. The electronic transmission functions are computed for a four-terminal CNT junction and two-terminal CNT systems using the Green's function method.[30] The CNT diameters in our simulations reach the range from 1.1 to 1.9 nm within which the growth distribution of CNTs can be controlled.[31] The transport calculations suggest that the TM linker atom enhances the intertube transport significantly and lowers the transport through a CNT only a little. Remarkably, the transmission function around the Fermi level and therefore also the conductance of the CNT junction depend strongly on the diameters of the CNTs. In addition, transport in a nanotube with a Cr atom or a Cr-benzene precursor molecule is studied. These systems are also experimentally relevant.[27] Larger decreases in the transmission function are observed in our results if there is only a Cr atom without a benzene molecule attached to a carbon ring of the nanotube. Thus, high concentrations of especially adsorbed (and possibly oxidized) Cr atoms should be avoided, e.g., by sputtering the Cr treated CNT networks.[28]

The structure of this article is as follows. In Sec. II, a short description of electronic transport calculations is presented. Thereafter, the systems investigated in this work are shown in Sec. III. The optimized structure of a CNT junction with a TM linker atom and the electronic transmission functions for those systems are considered in Sec. IV. In addition, Sec. IV deals with single CNTs with an adsorbed atom or a precursor molecule and presents transmission functions for CNT junctions where the size of the nanotubes is varied. In the same section, projected densities of states (PDOSs) for the linker atoms and charge transfer in the junction region are considered for analyzing the electron transport results. Finally, the results are summarized and the conclusions from the transport calculations are presented in Sec. V.

II. COMPUTATIONAL METHODS

The calculations of the present study are carried out with the FHI-aims electronic structure code package.[32] The basis functions in the FHI-aims code are numeric atom-centered orbitals and all the electrons in the system are treated self-consistently in the calculation. An important benefit of these orbitals is that the most time-consuming parts of the computations scale linearly with the number of atoms, which improves the performance of the code. The PBE exchange-correlation functional is used in the calculations.[33] The van der Waals interactions play a significant role in the formation of CNT junctions and we take them into account in the calculation as described in Ref. 34. To benchmark our electronic structure calculations, we have calculated the electronic and ionic structures of the bis(benzene)chromium molecule and compared the results with the literature.[35,36] Our approach reproduces well the previous findings including the large highest occupied-lowest unoccupied molecular orbital (HOMO-LUMO) band gap reflecting the closed-shell structure and small configuration mixing in multi-configuration calculations. Before the actual transport calculation, the atoms in the junction region are relaxed until the largest force component on all the atoms decreases below 10^{-2} eV/Å. The same force tolerance is used when the atoms in a CNT with an adsorbed chromium atom or a precursor molecule are relaxed.

Periodic boundary conditions are used in the electronic and ionic structure calculations. When describing CNT junctions, a supercell contains two perpendicular CNTs and their junction so that a periodic grid is formed. A vacuum layer of 50 Å is added between two parallel grids so that there is no coupling between them. In the case of single CNTs, a square lattice of infinitely long and parallel nanotubes is used with 50 Å vacuum between the adjacent CNTs. The Γ-point is used for k-point sampling, an approximation which gives accurate results because the number of CNT unit cells in one supercell is large enough. The number of carbon atoms corresponding to the part of one CNT in the supercell is considered in Sec. III.

In this work, the electronic transmission functions are computed for four-terminal CNT junction and two-terminal CNT systems using the Green's function method.[30] The main idea of our transmission modeling is that our systems consist of a central scattering region and semi-infinite leads. Transport calculations are performed with the transport module included in the FHI-aims code package.[18] The CNT junction system with four terminals is illustrated in Fig. 1. Single CNTs with either one Cr atom or a precursor molecule (see Figs. 2(a) and 2(b)) have two semi-infinite leads connected to the scattering region. It is assumed that the boundaries between the leads and the scattering region are non-reflecting. Then, the retarded Green's function of the scattering part of the system, when connected to the leads, can be calculated by solving the equation[18]

$$\left\{E - \hat{H}_0 - \sum_i \Sigma_i^r(E)\right\} G^r(\mathbf{r},\mathbf{r}';E) = \delta(\mathbf{r}-\mathbf{r}'), \qquad (1)$$

where E is energy, $\hat{H}_0$ the Hamiltonian of the scattering region, and Σ_i^r the self-energy of the i'th lead. It should be noted

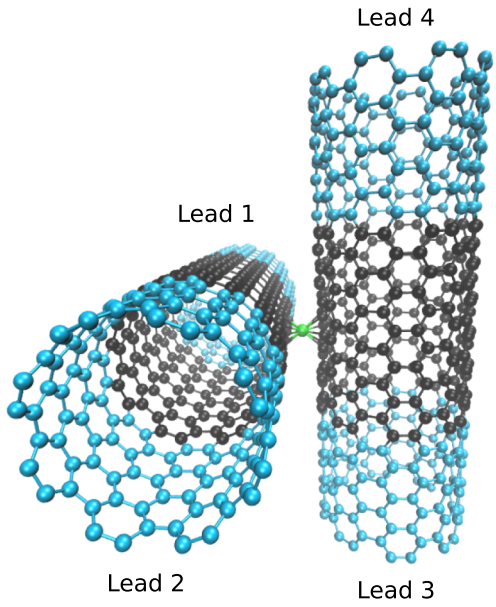

FIG. 1. Geometry of a CNT junction where two (8,8) CNTs are linked by a single Cr atom. The structure shown here is the minimum energy configuration given by the relaxation calculations. The scattering region of the transport calculation is indicated by black atoms and the CNT ends shown as light blue atoms belong to the semi-infinite leads.

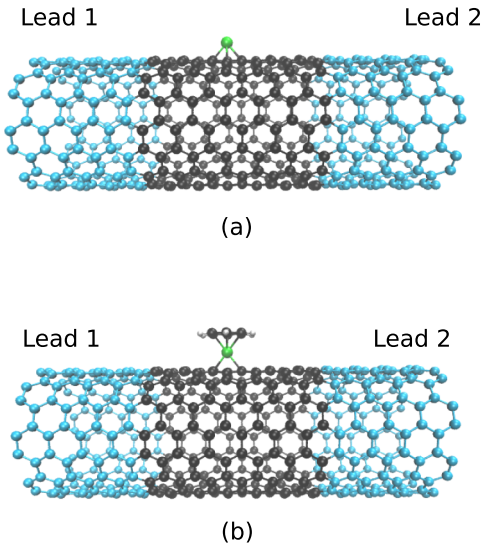

FIG. 2. Schematic figures of two CNTs with an adsorbed atom or an organometallic molecule. (a) A CNT with a single Cr atom and (b) a CNT with a Cr-benzene molecule. The scattering region of the transport calculation is indicated by black atoms and the CNT ends shown as light blue atoms belong to the semi-infinite leads.

that Eq. (1) is written in a general coordinate system $(\mathbf{r}, \mathbf{r}')$ whereas in a DFT code the operators and Green's functions are replaced by matrices in the basis of numerical atomic orbitals. The equation for the Green's function G^r requires constructing the Hamiltonian $\hat{H}_0$ for the scattering region. The Hamiltonian $\hat{H}_0$ is obtained by a DFT calculation for a periodic structure as described above. The terms $\Sigma_i^r(E)$ are the self-energies of the semi-infinite leads. To compute the self-energy, a standard DFT calculation of the periodic infinite CNT lead is performed and the Green's function for the semi-infinite lead is solved iteratively.[37]

As described above, ground state DFT calculations with periodic boundary conditions have to be carried out for the scattering region as well as for the infinite leads also before solving the retarded Green's function G^r. The energy levels of the ground-state solutions have to be correctly aligned in order to compute the transmission functions for the whole scattering region-leads systems. The carbon 1s energy eigenvalues of the atoms in the lead region are used as the energy reference in the alignment.

The transmission function for a single CNT or a CNT junction between leads i and j is given by[18]

$$T(E)_{i-j} = \int_{\partial\Omega_i}\int_{\partial\Omega_i}\int_{\partial\Omega_j}\int_{\partial\Omega_j} d\mathbf{r}_i d\mathbf{r}'_i d\mathbf{r}_j d\mathbf{r}'_j \times \Gamma_1(\mathbf{r}_i,\mathbf{r}'_i) G^r(\mathbf{r}'_i,\mathbf{r}_j) \times \Gamma_2(\mathbf{r}_j,\mathbf{r}'_j) G^a(\mathbf{r}'_j,\mathbf{r}_i). \quad (2)$$

In Eq. (2), the retarded Green's function G^r is a solution to Eq. (1) and the advanced Green's function G^a is the Hermitian conjugate of G^r. The Γ functions are given by the relation $\Gamma_i = \mathrm{i}(\Sigma_i^r - \Sigma_i^a)$, where Σ_i^a is the Hermitian conjugate of Σ_i^r, and describe the coupling of the semi-infinite leads to the scattering region.

It is possible to calculate the conductance of a nanotube or a nanotube junction with the Landauer formulation. If there is no bias between the leads and the system is at zero temperature, the conductance G reduces to[30],

$$G = \frac{2e^2}{h} T(E_\mathrm{F}), \quad (3)$$

where e is the elementary charge, h the Planck's constant, and $T(E_\mathrm{F})$ the value of the transmission function at the Fermi energy. If there is a finite bias over the scattering region, a self-consistent non-equilibrium calculation of the electronic structure is needed and the transport calculation becomes more complicated.[37] Then, it is also possible to determine an $I(V)$ curve for the system. In this work, the transport is considered only in a system which has a zero bias.

The results from the transport calculations are analyzed in Secs. III–V using the ground-state PDOSs and wavefunctions obtained with periodic boundary conditions. The transmission functions can be interpreted using them although one has to bear in mind that they are directly affected by the periodicity and in practice also by the k-point sampling. In contrast, the transmission functions, although calculated with some input from periodic calculations, correspond due to the use of the Green's function formalism directly to the systems of the scattering regions connected to the semi-infinite leads.

III. EXAMINED SYSTEMS

The nanotube junctions considered in this work consist of two perpendicular single-wall armchair CNTs that are connected by a TM atom. A schematic figure of a CNT junction with a Cr linker atom is presented in Fig. 1. A junction that consists of two (8,8) CNTs is primarily studied. However, the effect of the diameter of a nanotube on the transport is examined by computing electronic transmission functions for a smaller and a larger junction. The smaller junction has two (5,5) CNTs and the larger junction consists of (11,11) CNTs. The CNTs include 14 unit cells in periodic calculations so that the number of carbon atoms in one (5,5), (8,8), and (11,11) nanotube supercell is 280, 448, and 616, respectively. The first and last four unit cells of the CNTs belong in the Green's function transport calculations to the semi-infinite leads. The lead parts can be seen from Fig. 1.

The atoms of the CNT unit cell and its lattice vectors are relaxed before the junction is constructed. Then, the coordinates of the atoms in the supercell of the junction system are determined based on the relaxed CNT unit cell. Finally, all the atoms in the junction system up to the lead atoms are relaxed. In order to use the preconstructed Green's functions, the leads have to keep their ideal shape in transport calculations and therefore the relaxation of the lead atoms of the total system is not carried out.

To find the optimal structure of a CNT junction, the distance between the nanotubes is varied by first moving the frozen lead atoms of the two nanotubes with respect to each others. Then, the junction region in each configuration is relaxed separately. The total energy as a function of the nanotube distance is obtained and a second-degree polynomial is fitted to the total energy values. The polynomial fit gives the optimal distance between the CNTs. Here the nanotube

distance d_{tubes} is defined as

$$d_{\text{tubes}} = d_{\text{a}} - r_1 - r_2, \tag{4}$$

where d_{a} is the distance between the nanotube center axes, r_1 the radius of the first pristine nanotube, and r_2 that of the second pristine nanotube. It is important to place the TM atom precisely between the CNTs so that the linker atom lies above the center of a carbon hexagon. This can be done by rotating the CNTs around their axes to the correct axial angle before the relaxation calculation.

Electronic transport is also investigated in CNTs that have either a single Cr atom or a Cr-benzene organometallic molecule on top of the nanotube. It is important to understand the effect of an extra Cr atom on the transport in a CNT because part of the chromium atoms may bind to the outer wall of a CNT in the metal deposition process. In addition, a junction where two CNTs are linked by a TM atom can be made by using precursor molecules.[38] A precursor molecule can consist, for example, of a benzene molecule with a TM atom above the benzene ring. This precursor can attach to a CNT and the benzene ring can then be changed to another nanotube, which leads to a system where a TM atom connects two CNTs. In Figs. 2(a) and 2(b), two different CNT systems with an adsorbed atom or a molecule are presented. The CNTs in the systems are (8,8) nanotubes which include 14 unit cells each. The first and last four unit cells belong to the lead regions in the Green's function transport.

IV. RESULTS AND DISCUSSION

A. Structure of the TM-atom—CNT junctions

The optimized distance between the two CNTs in a junction depends on the sizes of the nanotubes and on the TM linker atom. The distances calculated according to Eq. (4) are listed in Table I for different CNT junctions. A single Cr atom increases the distance between the (5,5) and (8,8) CNTs only a bit compared with the junction without a linker atom. In contrast, the internanotube distance increases clearly more when a Mo or a W atom is placed in the junction.

A linker atom between the (8,8) CNTs pushes the neighboring carbon atoms towards the axes of the nanotubes and makes the nanotube sidewalls a little flatter. However, the changes are rather small and on the scale of Fig. 1 one cannot see noticeable deformation in the sidewalls of the CNTs. The structural rehybridization is known to be quite small in the bis(benzene)Cr molecule.[28] Similarly, the Cr atom does not cause remarkable changes in the different junctions investigated in this work. The average displacement of the six carbon atoms to which the Cr linker atom binds is approximately 0.19 Å towards the nanotube axis. In the relaxed geometry, the distance between the chromium and a carbon atom is 2.1 Å. This is smaller than the bond length calculated in Ref. 29, where the C-Cr distance is 2.34 Å. The experimentally determined distance between a chromium and a carbon atom is 2.15 Å in the bis(benzene)Cr molecule.[39] This value is remarkably close to that of the present study. Larger linker atoms also move the neighboring carbon atoms away from the TM atom and the average displacement of the six nearest-neighbor carbon atoms is 0.15 Å in the case of a molybdenum or tungsten linker atom. Around a given (8,8) junction, all the C-Mo and C-W bond lengths are similar and their mean value is 2.3 Å.

TABLE I. Minimum energy distances between two (5,5), (8,8), or (11,11) CNTs with and without a linker atom.

	Nanotube distance (Å)		
Linker atom	(5,5) CNTs	(8,8) CNTs	(11,11) CNTs
No linker	2.73	2.46	2.22
Cr	2.82	2.56	2.19
Mo	...	2.99	...
W	...	2.99	...

Decreasing the size of the nanotube results in a larger distance between CNTs. For a junction consisting of two (5,5) nanotubes and a Cr linker atom, the optimized distance between the nanotubes is 2.82 Å. The same distance in a junction where two (11,11) CNTs are linked by a Cr atom is 2.19 Å so that the nanotubes in this case are closer to each other than in the (8,8) junction with a Cr atom. The distance between the CNTs decreases in the case of (5,5) and (8,8) junctions when the Cr linker atom is removed. In contrast, the (11,11) junction has a larger distance between the CNTs without the Cr atom. This is related to the small curvature of an (11,11) nanotube.

The bond lengths between the linker atom and the nearest carbon atoms are around 2.2 Å in (5,5) and (11,11) junctions. When the curvature of the nanotube is large ((5,5) junction), two bonds between the Cr and the carbon atoms are approximately 0.1 Å longer than the other four bonds. In a larger (8,8) junction, the difference between the short and long bonds in the junction region is 0.07 Å. The lengths of the bonds between the Cr atom and the nearest carbon atoms in the (11,11) junction vary only 0.03 Å.

In conclusion, Cr is a more favourable linker atom than Mo or W, because its introduction into the junction does not cause a large outward relaxation of the two CNTs. Indeed, experimentally Cr is found to enhance the conductivity of the CNT network more than Mo and W. Below, we find that the influence of the Cr, Mo, and W linker atoms on the electron transmission functions is very similar so that the different conductivity enhancement is most probably related to the ease of introduction of the linker atom to the junction. Moreover, the atomic relaxations indicate that the increase of the CNT radius favors the incorporation of Cr into the junction.

In order to quantify the strength by which a Cr atom binds two CNTs together, we calculate the binding energies for a Cr atom adsorbed on a CNT and for a Cr atom placed between two CNTs. The binding energy for a Cr atom on a nanotube is given by

$$E_{\text{b},1} = E_{\text{T}}[\text{CNT-Cr}] - E_{\text{T}}[\text{CNT}] - E_{\text{T}}[\text{Cr}], \tag{5}$$

where E_{T}[CNT-Cr] is the total energy of an (8,8) CNT with an adsorbed Cr atom, E_{T}[CNT] the total energy of an (8,8) CNT, and E_{T}[Cr] the total energy of a Cr atom. The value of $E_{\text{b},1}$ is +0.2 eV indicating that an adsorbed Cr could be slightly instable according to our DFT results. One can also calculate the binding energy for a Cr atom linking two perpendicular CNTs, which can be expressed as

$$E_{b,2} = E_T[\text{CNT-Cr-CNT}] - E_T[\text{CNT}] - E_T[\text{CNT-Cr}], \quad (6)$$

where E_T[CNT-Cr-CNT] is the total energy of a Cr-(8,8) CNT junction. The binding energy $E_{b,2}$ is approximately −4.2 eV reflecting a clear stability of the closed-shell electronic configuration.

B. Effect of the TM atom on electron transport through CNT junctions

Calculations of the PDOSs for the group 6 TM linker atoms in a CNT junction show that both spin channels are equal reflecting the closed-shell structure of the TM atom between two benzene rings (see Figs. 6 and 7). Hence, the spin dependence is neglected in these transport calculations. Electronic transport is studied both for an empty CNT junction and in a junction with a TM linker atom. By symmetry, the intratube transmissions along both CNTs (between leads 1 and 2 or between leads 3 and 4) are equal. Additionally, the intertube transport computed from lead 1 to lead 3 coincides with that from lead 1 to lead 4. Therefore, intertube transport is discussed here only between the leads 1 and 3 and intratube transport between the leads 1 and 2.

Transmission functions for intratube and intertube transport for a junction where the chirality of both CNTs is (8,8) are shown in Figs. 3(a) and 3(b), respectively. Intratube transport in a CNT junction without a TM linker atom resembles that of an isolated armchair CNT and only minor details are affected by the neighboring nanotube. When a TM linker atom is added between the CNTs, a few small dips appear in the intratube transmission function reflecting a slightly increased perturbation. The transmission at the Fermi level remains almost the same as the transmission for an isolated nanotube.

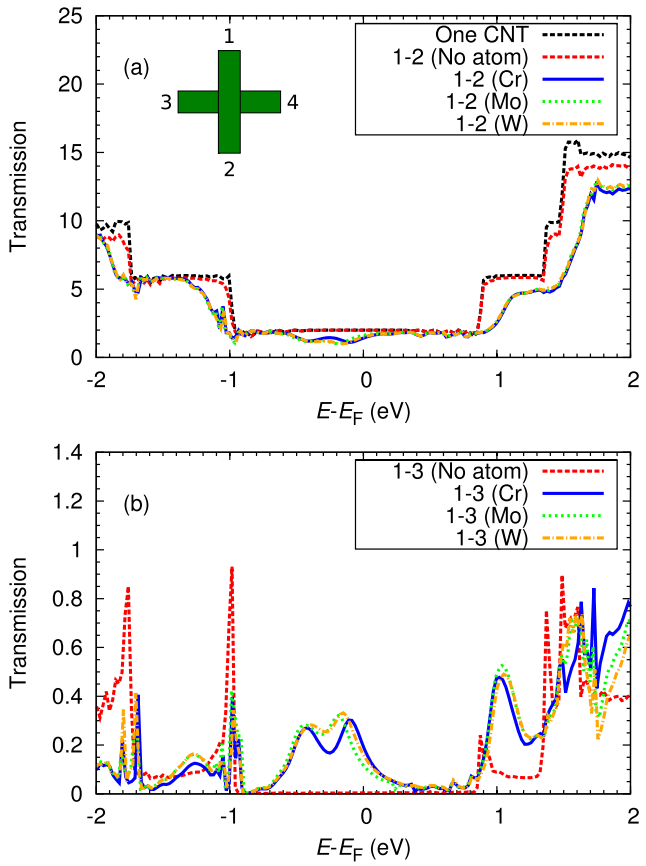

FIG. 3. (a) Intratube (lead order 1-2) and (b) intertube (lead order 1-3) transmission functions for an (8,8) CNT junction without a linker atom and for a CNT junction with a Cr, Mo, or W atom. The black dashed line in the upper plot shows the transmission function for a pristine isolated (8,8) CNT. The inset in the upper plot is a schematic CNT figure with the lead numbering.

As shown in Fig. 3(b), without a linker atom, the intertube transport practically vanishes over a wide range of about 2 eV around the Fermi level. There are high peaks corresponding to the openings of new transmission channels in intratube transmission and the ensuing high densities of states. The behavior of the intertube transmission function for a junction without a TM atom is similar to the transmission function obtained in an earlier work.[18]

The intertube transport is clearly enhanced by the TM atom in the junction as shown in Fig. 3(b). All three different linker atoms increase the transmission within the important energy region of $E - E_F = -0.8$ eV to $+0.2$ eV by giving rise to two broad peaks below the Fermi energy E_F. The peaks are rather symmetric and the tail of the peak located closest to the Fermi level extends above it. The transmission lowers at energies above these two peaks but rises again at about 0.8 eV above the Fermi level in the region of two transmission channels along a CNT. According to the calculations, all the three TM atoms examined in this work seem to improve the intertube transport equally well.

Our transmission curves differ from those obtained in Ref. 29, where the transmission peaks are significantly broader and the transmission is larger in magnitude. The broad transmission peaks of Ref. 29 also extend with larger intensities further above the Fermi level. However, those transmission functions have been calculated for two parallel and semi-infinite (5,5) CNTs linked with a metal atom so that the clear differences with respect to our system geometry seem to affect quite remarkably the intertube transmission. The conductance of a CNT junction is known to depend on the angle between the nanotubes.[13–15] Thus, in addition to different tube radii (see the discussion below), the effects due to the reflections at the tube ends (causing quasilocalized end states) and the angle dependence are explanations for the differences between the transmission functions of the present and earlier studies.

C. Effect of the CNT radius on electron transport through TM-atom—CNT junctions

According to the structure optimizations of CNT junctions, the size of the nanotubes affects the distance between them remarkably as well as the distribution of TM-atom–C distances (Sec. IV A). To investigate how electronic transport depends on the diameter of nanotubes, transmission functions are computed for two other junctions in addition to the (8,8) CNT junction. One junction consists of two (5,5) CNTs and the other contains two (11,11) CNTs. The linker atom in these junctions is always Cr. Transmission functions for intratube and intertube transport in the three different junctions are presented in Figs. 4(a) and 4(b), respectively.

In the case of intratube transport shown in Fig. 4(a), the transmission function shows a region of two slightly perturbed transmission channels. This region lies quite symmetrically

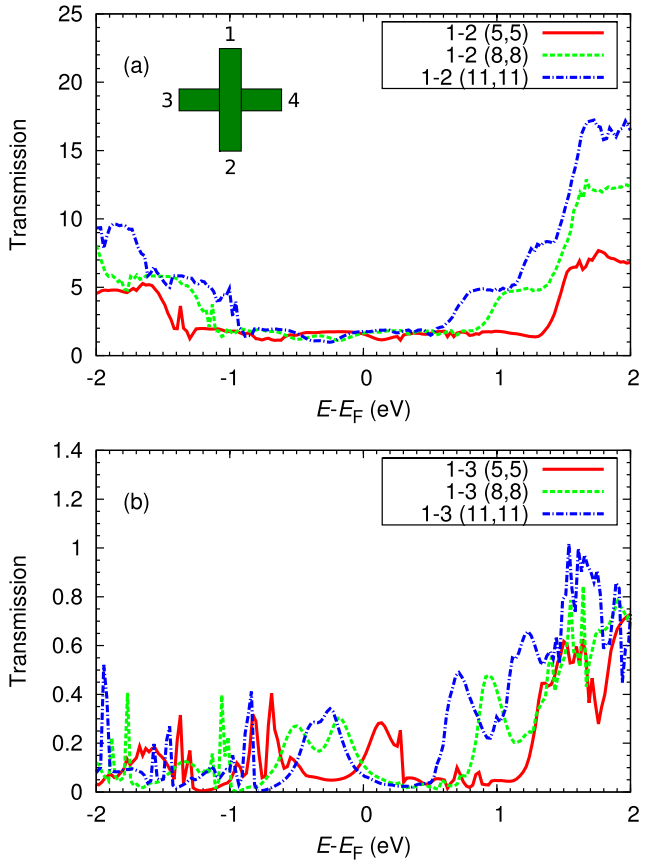

FIG. 4. (a) Intratube (lead order 1-2) and (b) intertube (lead order 1-3) transmission functions for junctions corresponding to CNTs of different radii. In the upper plot, an inset describing the lead numbering is shown.

with respect to the Fermi energy. Due to the quantization around the tube circumference, the width of this energy region increases with the decreasing diameter of the nanotube. The other CNT and the Cr linker atom lower the transport along one nanotube to some extent but the conductance of one nanotube remains near that of a pristine CNT.

Intertube transmission functions close to the Fermi level (Fig. 4(b)) are clearly affected by the radii of CNTs. When the junction consists of two perpendicular (11,11) CNTs, a double peak structure below the Fermi energy can be seen in the intertube transmission function. Decreasing the radius of the nanotube increases the distance between the peaks. In the case of the small (5,5) CNTs, the peaks are separated even more so that the peak closest to the Fermi level has moved above it. Moreover, a few other smaller peaks appear next to the widely separated peaks in the intertube transmission function for the (5,5) CNT junction. When the curvature of the nanotube increases, the transmission near the Fermi level changes significantly. Thus, the radii of CNTs have a large effect on the conductance of the CNT junction.

D. Transmission functions for a CNT with an adsorbed TM atom or a precursor molecule

TM atoms can bind to the surface of a CNT, which affects the transport through a single CNT. In reality, the adsorbed TM atom may be easily further oxidized. To examine the impact of a single adsorbed atom or a molecule on the transport through a nanotube, electronic transmission functions are computed both for an (8,8) CNT with a Cr atom and with a Cr atom that connects a benzene molecule to the nanotube. Transmission functions for these two systems and a pristine (8,8) CNT are compared in Fig. 5.

It can be seen from the transmission function for a CNT with an adsorbed Cr atom that the values near the Fermi level decrease significantly. Thus, the Cr atom causes scattering as Fano antiresonances related to localized states at the Cr atom.[40] The two transmission curves for the two spin channels are quite similar but there are, however, differences between them. The transmission function for the first spin channel has dips below the Fermi level whereas the second spin channel shows dips mainly above the Fermi energy reflecting the different positions (and occupancies with the total magnetic moment of $4\mu_B$) of the opposite spin states. If there is also a benzene molecule attached to the Cr atom, the transmission function is spin independent and it only has one clear dip below the Fermi energy and the values of the function remain almost as good as those of a pristine nanotube. In conclusion, adsorbed atoms lower significantly the intertube transport in the CNT network. This is certainly true for a high concentration of them, in which case also the relative distances between the adsorbates play an important role.[41,42] Thus, it is important to get rid of the strongly adsorbed atoms or molecules when processing conductive CNT networks.

E. Projected density of states for linker and carbon atoms at TM-atom—CNT junctions

The enhancement in the intertube transmission curves below the Fermi level in Fig. 3(b) is related to the PDOS at the TM atom site. The PDOS computed for the Cr atom linking two (8,8) CNTs shows one very sharp and high peak located near the Fermi level (see Fig. 6). In addition, there are more broader and lower peaks which are between 0.3 eV and 1.2 eV below the Fermi level. All these peaks are related to the TM

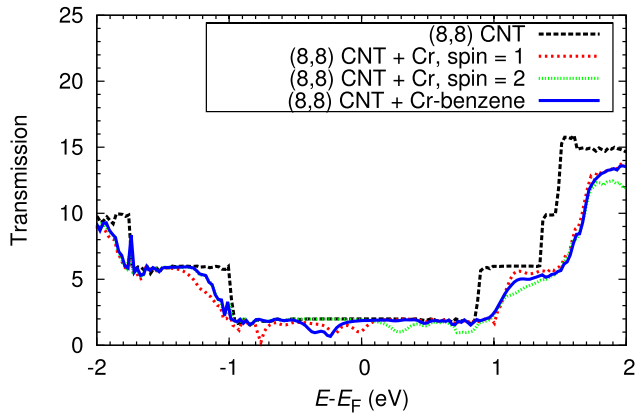

FIG. 5. Transmission functions for a pristine (8,8) CNT, for an (8,8) CNT with a Cr atom, and for an (8,8) CNT with an organometallic molecule consisting of a benzene ring and a Cr atom. In the case of the (8,8) CNT with a Cr atom, the transport is spin-dependent and transmission functions are shown for both spin channels.

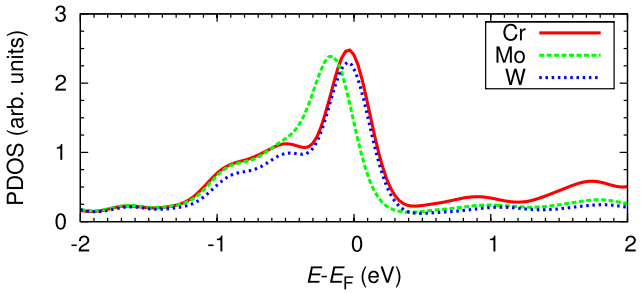

FIG. 6. Projected densities of states for group 6 TM linker atoms in a TM atom-(8,8) junction.

atom d-states hybridized with carbon valence states. By comparing the intertube transmission curves with the PDOS plot, it can be observed that the two jumps in the intertube transmission in Fig. 3(b) appear nearly at the same energy values as the region of enhanced density of states in the PDOS plot for the Cr linker atom.

The carbon atoms to which the TM atoms are bound have quite different PDOS curves. The PDOSs for carbon atoms in two different systems are presented in Fig. 7. The first system is a Cr-(8,8) CNT junction that is schematically illustrated in Fig. 1, and the carbon atom for which the PDOS is shown is one of the nearest neighbors of the Cr linker atom. The other system is a pristine (8,8) CNT. In the regime between $E - E_F \approx -1$ eV and $E - E_F \approx 0$ eV the PDOS for the junction is enhanced compared with the PDOS for a pristine CNT. The enhancement in the transport can only occur when the peaks in the PDOS of the Cr atom are located at the same positions as those of the different carbon atoms. The PDOS for the other 11 neighboring carbon atoms is similar to the red curve shown in Fig. 7. However, the intensities of individual peaks can be different due to the inequivalency of the carbon atoms.

A sharp peak is also seen at the Fermi level in the PDOS plots when the Cr atom is changed to a Mo or a W atom. Moreover, there is always a region just below the Fermi energy showing an increase in the PDOS so that the type of the linker atom does not affect the behavior of the PDOS curve near the Fermi level. Instead, a few peaks located above the Fermi level move towards higher energies. The states corresponding to these peaks are located far from the Fermi level and therefore do not have an influence on the conductance of the junction for relevant bias voltages.

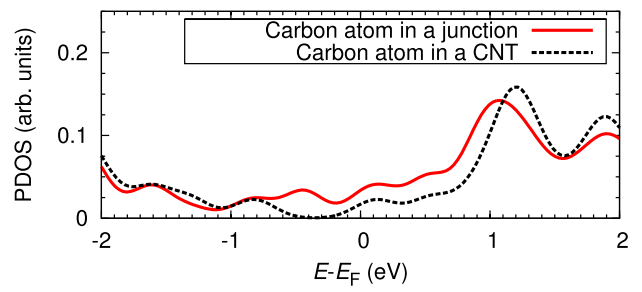

FIG. 7. Projected density of states for a carbon atom bound to the Cr atom in a Cr-(8,8) CNT junction (red solid line) and for a carbon atom in an (8,8) CNT (black dashed line). The carbon atom in the Cr-(8,8) CNT junction is one of the nearest neighbors of the Cr linker atom.

F. Charge densities and charge transfer at the TM-atom—CNT junction

It is possible to study the effect of a TM atom on the conductance of a CNT junction also by examining electron densities of various eigenstates around the Fermi energy regime. Since the intertube transmission function increases significantly between $E - E_F \approx -0.8$ eV and $E - E_F \approx 0.2$ eV, the electronic states close to these energies are of great importance. The electron densities of an unoccupied low-energy eigenstate ($ULEE_1$) and the three occupied high-energy eigenstates ($OHEE_1$, $OHEE_2$, and $OHEE_3$) of a Cr-(8,8) CNT junction are drawn in Figs. 8(a)–8(d). The states correspond to the Γ point of the supercell Brillouin zone. The isodensity for the orbital plotting has the same value in all plots. The energy of the $ULEE_1$ is about 0.1 eV above the Fermi energy. The $OHEE_2$ and $OHEE_3$ are approximately 0.4 eV and 0.6 eV below the Fermi energy, respectively, and the energy of the $OHEE_1$ at the Fermi level.

The electron density of the $ULEE_1$ is rather low close to the Cr atom as shown in Fig. 8(d) and the Cr orbitals do not seem to couple strongly to those of carbon atoms in the nanotubes. This can also be seen from the PDOS for the Cr and carbon atoms which do not overlap (Figs. 6 and 7). The electron density is more localized for the $OHEE_1$, $OHEE_2$, and $OHEE_3$ orbitals than for the $ULEE_1$ orbital. The $OHEE_1$ orbital shows a toroidal $3d_{z^2}$ shape (see Fig. 8(c)) surrounding the Cr linker atom. However, it exhibits no significant coupling between the chromium and carbon orbitals. Considering the electron densities of the $OHEE_2$ and $OHEE_3$, orbitals of both CNTs hybridize strongly with the Cr atom orbitals. A similar coupling between the carbon π orbitals and d orbitals of the Cr atom has been seen in a system consisting of two polyacene molecules connected by one Cr atom,[29] which explains the good conductivity of the system. The $OHEE_2$ and $OHEE_3$ orbitals contain four small longitudinal regions that extend from one CNT to the other. Additionally, the charge density near a few carbon atoms is increased by the Cr linker atom. In order to understand the formation of the Cr-(8,8) CNT junction states shown in Fig. 8, we have considered the electronic orbitals of the bis(benzene)Cr molecule calculated by the FHI-aims code. The HOMO $a_{1g}(\sigma)$ (for the notation, see, e.g., Ref. 35) corresponds to the state $OHEE_1$ and the HOMO-1 $e_{2g}(\delta)$ to the states $OHEE_2$ and $OHEE_3$. The counterpart of the $ULEE_1$ state is the LUMO e_{2u} which is localized in the benzene rings with minimum hybridization with Cr orbitals.

An enhanced electron density in the junction region indicates that orbitals such as $OHEE_2$ and $OHEE_3$ result in an improvement in the conductivity as shown in the intertube transmission function. This means that the increase in the transmission curve at $E - E_F \approx -0.8$ to $+0.2$ eV in Fig. 3(b) is related to these kinds of states. $OHEE_2$ and $OHEE_3$ states correspond to the two lower intensity peaks in this energy region in the PDOS for the Cr atom in Fig. 6. The narrow PDOS peak in Fig. 6 signalizes a localized state, i.e., it corresponds to the $OHEE_1$ state and these states do not induce a transmission peak.

Connecting the two CNTs with a TM atom causes some charge transfer between the atoms in the junction region. According to the Hirshfeld charge analysis, the linker atom

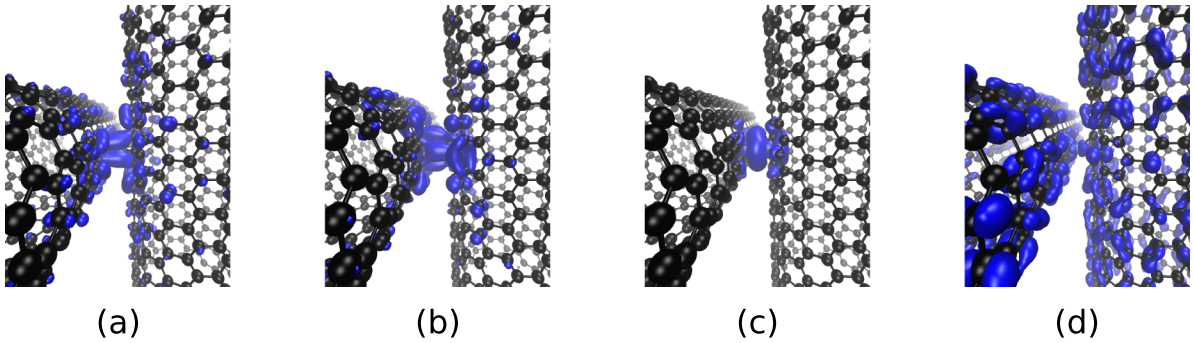

FIG. 8. Charge densities of (a) the $OHEE_3$, (b) the $OHEE_2$, (c) the $OHEE_1$, and (d) the $ULEE_1$ eigenstates (see the text) for the Cr-(8,8) CNT junction. The charge density is represented by a blue isosurface which has the same value in all plots. The energy of the orbitals increases from left to right.

obtains a small positive charge and its value for the Cr, Mo, and W atom is 0.06, 0.29, and 0.17, respectively. In the CNTs, the donated charge is spread over a few bond distances from the junction and the sign of the Hirshfeld charge oscillates between neighboring C atoms. In a recent experimental work by Tian *et al.*,[28] no significant charge transfer between a Cr atom and a CNT network has been observed, which is in agreement with the small Hirshfeld charge value for the Cr linker atom.

V. CONCLUSIONS

Electronic transport in a metallic CNT junction where two perpendicular nanotubes are linked by a TM atom (Cr, Mo, and W) has been investigated computationally. A benefit of our modeling is that the nanotubes are infinitely long and there are no reflections coming from the nanotube ends. Thereby, our model describes truly the properties of the junction itself.

The intertube transport is significantly enhanced by the linker atom. All the three linker atoms improve the intertube transport equally well and give rise to two broad peaks near the Fermi level in the transmission function. However, Mo and W linker atoms disturb the ionic structure of the pristine CNT junction more than Cr. Therefore, Cr can be more easily incorporated into the junction than Mo or W and the conductivity is expected to be the most enhanced due to Cr treatment. The size of a CNT has a significant effect on the transport through the junction. If the junction consists of small nanotubes, the transmission function is enhanced well above and well below the Fermi level. This results from the high curvature of the small nanotubes and the spreading of the hybridized TM atom—C states in energy.

A linker atom does not lower the intratube transport in a CNT junction remarkably. However, a Cr atom on top of a single nanotube lowers the transport through the nanotube more than in a CNT junction with a TM linker atom. An organometallic Cr-benzene molecule on a CNT also disturbs the transport but the depressions in the transmission function are smaller compared with those caused by a single Cr atom.

ACKNOWLEDGMENTS

We acknowledge the computational resources provided by CSC—IT Center for Science. Moreover, part of the calculations were performed using computer resources within the Aalto University School of Science "Science-IT" project. We thank Professor Kari Laasonen and Dr. Ari P. Seitsonen for useful discussions and comments. This work was supported by the Academy of Finland through its Centres of Excellence Programme (2012-2017) under Project No. 251748. We are also thankful for support from the Aalto Energy Efficiency (AEF) research programme.

[1]E. Artukovic, M. Kaempgen, D. S. Hecht, S. Roth, and G. Grüner, Nano Lett. **5**, 757 (2005).
[2]Y.-M. Chien, F. Lefevre, I. Shih, and R. Izquierdo, Nanotechnology **21**, 134020 (2010).
[3]S. Kim, S. Kim, J. Park, S. Ju, and S. Mohammadi, ACS Nano **4**, 2994 (2010).
[4]Z. Yang, T. Chen, R. He, G. Guan, H. Li, L. Qiu, and H. Peng, Adv. Mater. **23**, 5436 (2011).
[5]S. Park, M. Vosguerichian, and Z. Bao, Nanoscale **5**, 1727 (2013).
[6]S. Kumar, J. Y. Murthy, and M. A. Alam, Phys. Rev. Lett. **95**, 066802 (2005).
[7]P. N. Nirmalraj, P. E. Lyons, S. De, J. N. Coleman, and J. J. Boland, Nano Lett. **9**, 3890 (2009).
[8]S. Seppälä, E. Häkkinen, M. J. Alava, V. Ermolov, and E. T. Seppälä, EPL **91**, 47002 (2010).
[9]P. E. Lyons, S. De, F. Blighe, V. Nicolosi, L. F. C. Pereira, M. S. Ferreira, and J. N. Coleman, J. Appl. Phys. **104**, 044302 (2008).
[10]K. Yanagi, H. Udoguchi, S. Sagitani, Y. Oshima, T. Takenobu, H. Kataura, T. Ishida, K. Matsuda, and Y. Maniwa, ACS Nano **4**, 4027 (2010).
[11]M. S. Fuhrer, J. Nygård, L. Shih, M. Forero, Y.-G. Yoon, M. S. C. Mazzoni, H. J. Choi, J. Ihm, S. G. Louie, A. Zettl, and P. L. McEuen, Science **288**, 494 (2000).
[12]F. A. Bulat, L. Couchman, and W. Yang, Nano Lett. **9**, 1759 (2009).
[13]T. Nakanishi and T. Ando, J. Phys. Soc. Jpn. **70**, 1647 (2001).
[14]A. Buldum and J. P. Lu, Phys. Rev. B **63**, 161403(R) (2001).
[15]A. A. Maarouf and E. J. Mele, Phys. Rev. B **83**, 045402 (2011).
[16]Y.-G. Yoon, M. S. C. Mazzoni, H. J. Choi, J. Ihm, and S. G. Louie, Phys. Rev. Lett. **86**, 688 (2001).
[17]M. Monteverde and M. Núñez Regueiro, Phys. Rev. Lett. **94**, 235501 (2005).
[18]P. Havu, M. J. Hashemi, M. Kaukonen, E. T. Seppälä, and R. M. Nieminen, J. Phys.: Condens. Matter **23**, 112203 (2011).
[19]S. B. Yang, B.-S. Kong, D.-H. Jung, Y.-K. Baek, C.-S. Han, S.-K. Oh, and H.-T. Jung, Nanoscale **3**, 1361 (2011).
[20]H.-Z. Geng, K. K. Kim, K. P. So, Y. S. Lee, Y. Chang, and Y. H. Lee, J. Am. Chem. Soc. **129**, 7758 (2007).
[21]S. Li, P.-X. Hou, C. Liu, T. Liu, W.-S. Li, J.-C. Li, and H.-M. Cheng, J. Mater. Chem. A **2**, 3308 (2014).
[22]S.-H. Ke, H. U. Baranger, and W. Yang, Phys. Rev. Lett. **99**, 146802 (2007).
[23]J.-W. Do, D. Estrada, X. Xie, N. N. Chang, J. Mallek, G. S. Girolami, J. A. Rogers, E. Pop, and J. W. Lyding, Nano Lett. **13**, 5844 (2013).
[24]R. A. Bell, M. C. Payne, and A. A. Mostofi, Phys. Rev. B **89**, 245426 (2014).
[25]K. H. Khoo and J. R. Chelikowsky, Phys. Rev. B **79**, 205422 (2009).
[26]C. F. McAndrew and M. Baxendale, Nanotechnology **24**, 305202 (2013).
[27]I. Kalinina, E. Bekyarova, S. Sarkar, F. Wang, M. E. Itkis, X. Tian, S. Niyogi, N. Jha, and R. C. Haddon, Macromol. Chem. Phys. **213**, 1001 (2012).

[28]X. Tian, M. L. Moser, A. Pekker, S. Sarkar, J. Ramirez, E. Bekyarova, M. E. Itkis, and R. C. Haddon, Nano Lett. **14**, 3930 (2014).
[29]E. Y. Li and N. Marzari, ACS Nano **5**, 9726 (2011).
[30]S. Datta, *Electronic Transport in Mesoscopic Systems* (Cambridge University Press, Cambridge, 1995).
[31]Y. Tian, M. Y. Timmermans, M. Partanen, A. G. Nasibulin, H. Jiang, Z. Zhu, and E. I. Kauppinen, Carbon **49**, 4636 (2011).
[32]V. Blum, R. Gehrke, F. Hanke, P. Havu, V. Havu, X. Ren, K. Reuter, and M. Scheffler, Comput. Phys. Commun. **180**, 2175 (2009).
[33]J. P. Perdew, K. Burke, and M. Ernzerhof, Phys. Rev. Lett. **77**, 3865 (1996).
[34]A. Tkatchenko and M. Scheffler, Phys. Rev. Lett. **102**, 073005 (2009).
[35]V. M. Rayón and G. Frenking, Organometallics **22**, 3304 (2003).
[36]I. S. Youn, D. Y. Kim, N. J. Singh, S. W. Park, J. Youn, and K. S. Kim, J. Chem. Theory Comput. **8**, 99 (2012).
[37]S.-H. Ke, H. U. Baranger, and W. Yang, Phys. Rev. B **70**, 085410 (2004).
[38]S. Sarkar, S. Niyogi, E. Bekyarova, and R. C. Haddon, Chem. Sci. **2**, 1326 (2011).
[39]A. Haaland, Acta Chem. Scand. **19**, 41 (1965).
[40]J. A. Fürst, M. Brandbyge, A.-P. Jauho, and K. Stokbro, Phys. Rev. B **78**, 195405 (2008).
[41]J. M. García-Lastra, K. S. Thygesen, M. Strange, and Á. Rubio, Phys. Rev. Lett. **101**, 236806 (2008).
[42]M. J. Hashemi, K. Sääskilahti, and M. J. Puska, Phys. Rev. B **83**, 115411 (2011).